Using Satellite Passive Microwave Data to Study Arctic Polar Lows

Elizaveta V. Zabolotskikh[1,2], Leonid P. Bobylev[1,3], Vladimir Kudryavtsev[1,2], and Leonid Mitnik[4]

[1]Nansen Centre, St. Petersburg, Russia
[2]Russian State Hydrometeorological University, St. Petersburg, Russia
[3]Nansen Centre, Bergen, Norway
[4]Pacific Oceanological Institute, FEB RAS, Vladivostok, Russia

European Polar Low Working Group Oslo Polar Low Workshop, 21-22 May 2012

Polar lows and their general characteristics

International Polar Year 2007-2008 initiated enhanced research activity on adverse weather in polar regions including polar lows in the Arctic sector of Atlantic Ocean

- Polar lows are short-living intense meso-scale maritime atmospheric low pressure weather systems, observed over high latitudes during wintertime
- Short lifetime: from several hours to 2 days (average 15÷20 hours)
- Small size: 100÷1000 км
- High surface wind speed: > 15 m/s (some time > 30 m/s)
- Typically marine phenomenon: polar lows rapidly break down over land and ice cover

Areas of occurrence of polar lows in the Arctic

Arctic polar lows significantly more intensive than Antarctic ones due to large fluxes of heat and moisture

Most intensive Arctic polar lows are called “Arctic hurricanes”

Nordic seas is one of the main genesis areas for polar lows in the Arctic

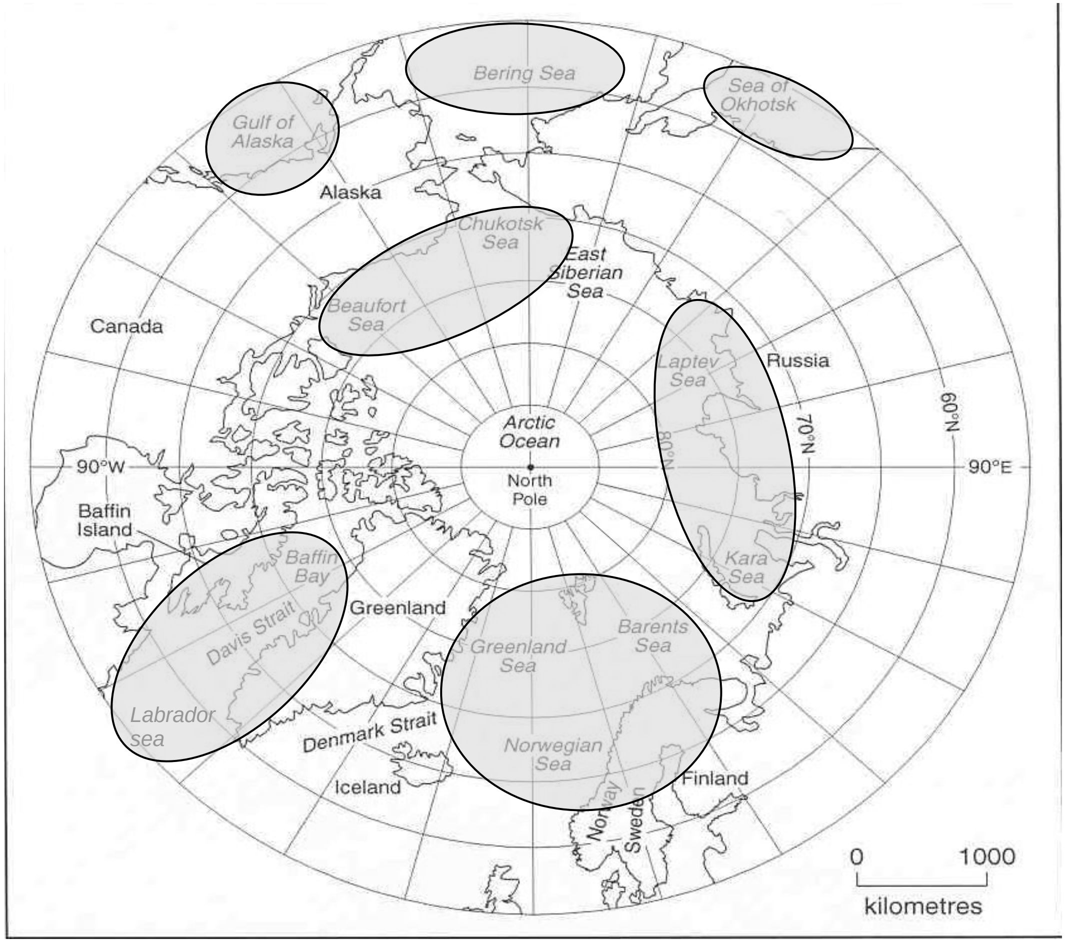

Polar lows – threat to man's activities in the Arctic

- Polar lows are associated with heavy snowfalls and high surface wind speed, possessing high destructive power
- They are one of the most frequent reason of ship icing
- Polar lows represent threat to such businesses as oil and gas exploitation, fisheries and shipping
- They can worsen because of shrinking Arctic sea ice due to global warming *(Erik Kolstad: "The bad news is that as the sea ice retreats you open up a lot of new areas to this kind of extreme weather")*

Are polar lows climatologically important?

- This issue is not clear now and more studies are needed to assess climatological importance of polar lows
- In any case, to be of climatological important, frequent occurrence of polar lows has to take place in considered area

- Hypotheses:

○ Individual polar lows can have fluxes of heat of up to 1 000 W/m^2, therefore loss of heat from ocean surface can trigger downward convection in ocean

○ Polar low can lead to ocean surface warming of more than 1 C within few hours due to turbulent entrainment of subsurface warm water core caused by strong wind. It may be potential positive feedback mechanism for cyclone intensity (*Saetra et al., Tellus, 60A, 2008*)

Earliest reference to polar lows and beginning of their satellite observations

One of earliest references to phenomenon known now as polar low was made by Peter Dannevig, who wrote about ‘instability lows’ over seas around Norway in book for pilots in 1954

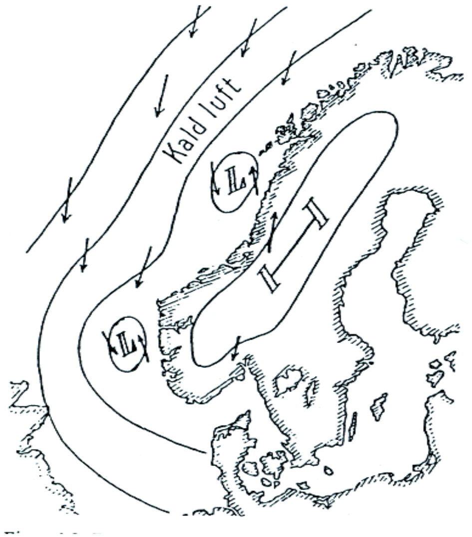

Dannevig's 1954 schematic surface chart showing two 'instability lows' within northerly outbreak of polar air near Norwegian coast

Since 1960s - general availability of satellite imagery

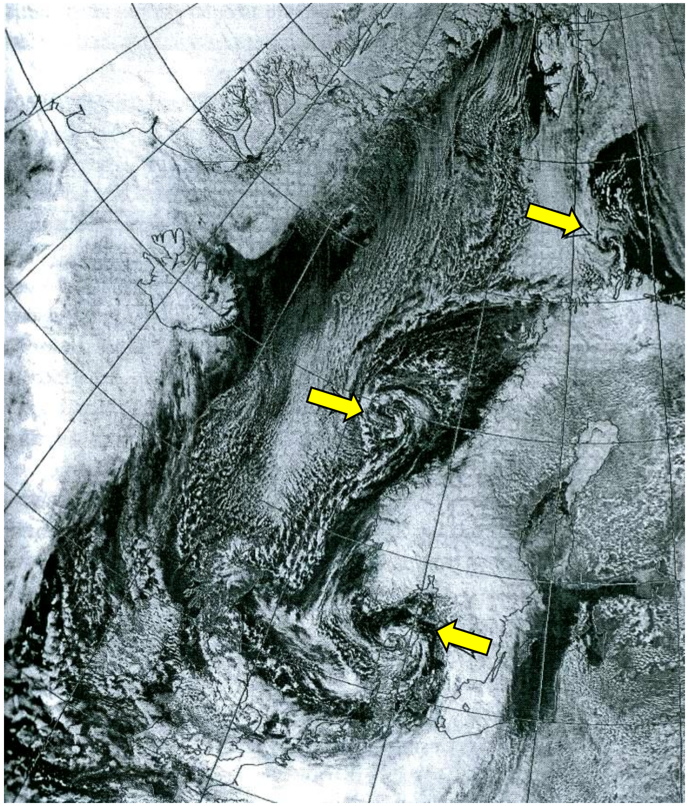

27 April 1985 13:08 UTC

Visible NOAA AVHRR image of polar air outbreak down coast of Norway and Denmark.

Three polar lows were formed at:

- North Cape
- Norwegian Sea at 65N
- over Denmark

Complications in polar low detection, tracking, study and forecasting

- Small size and short lifetime of polar lows makes them difficult to detect
- Sparse synoptic observations cannot provide sufficient data for modeling and forecasting
- Resolution of most numerical weather models is not sufficient for polar low study
- Most of the polar lows are not revealed on surface analysis maps

Polar lows - highly complicated phenomena: their study, timely detection, tracking and forecasting still is a challenge for Earth sciences

Example: Polar low over Norwegian Sea 30-31 January 2008

Surface analysis maps: this polar low is not found on weather charts issued by local weather bureaus

Polar low is detected at Envisat ASAR archive images. It arose on 30 and destructed on 31 Jan 2008

German National Meteorological Service, Hamburg Branch Office

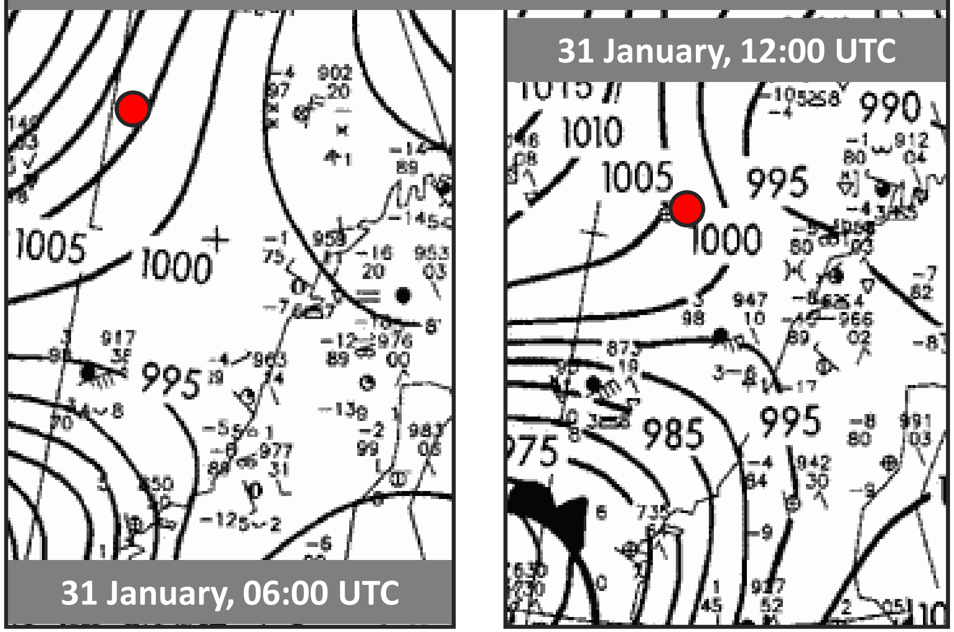

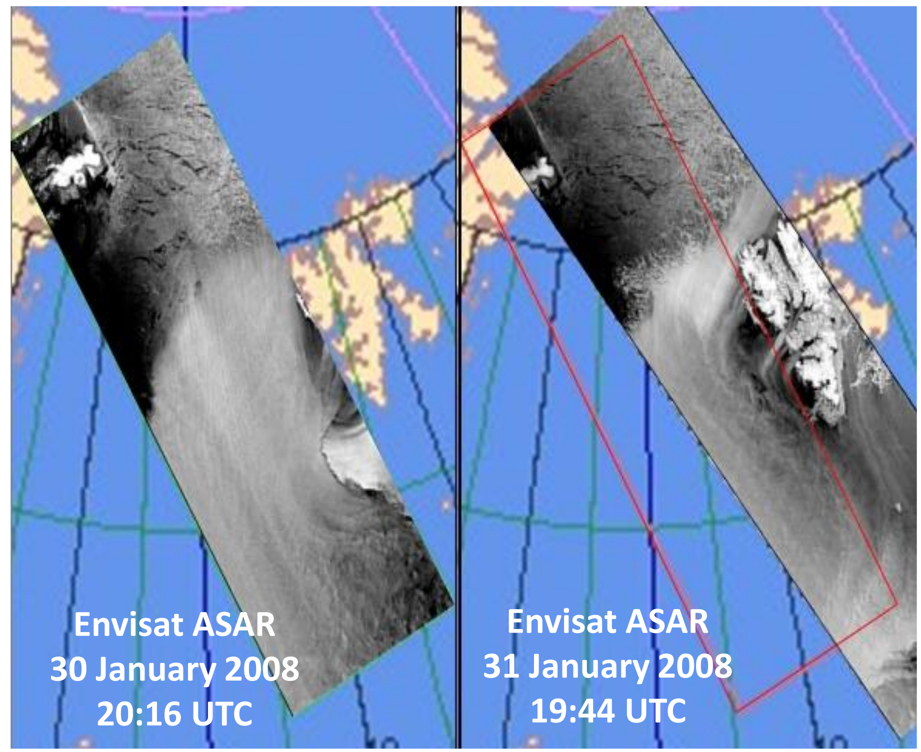

Arctic polar low observations from satellites: milestones

- **Infrared and visible observations during 1960s provided major advance in polar low study**
- **Low resolution sea surface wind field retrievals began in 1978 with first Ku-band scatterometer on board Seasat**
- **High resolution surface wind fields inside polar lows are available from spaceborne SAR since 1978 with the same satellite Seasat and from RAR since 1983 with Kosmos-1500 satellite**
- **Satellite passive microwave data, available since 1979 from SMMR, since 1987 from SSM/I and since 2002 from AMSR-E and AMSR are now one of the main sources of quantitative spatial information for polar lows study.**

Satellite observations in infrared and visible: polar low north to Norway on 26-27 February 1987

NOAA AVHRR IR (10.3-11.3 µm) images

**Development phase, 26 February 1987
04:28 UTC**

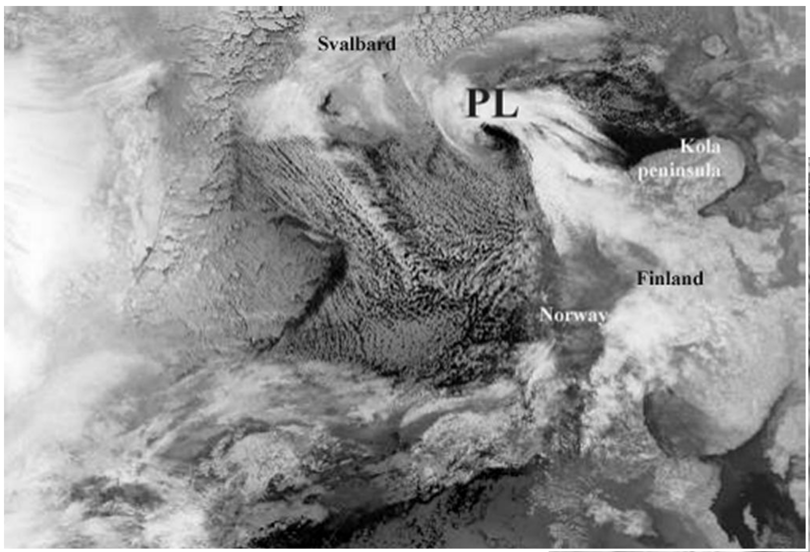

**Mature phase, 27 February 1987
04:18 UTC**

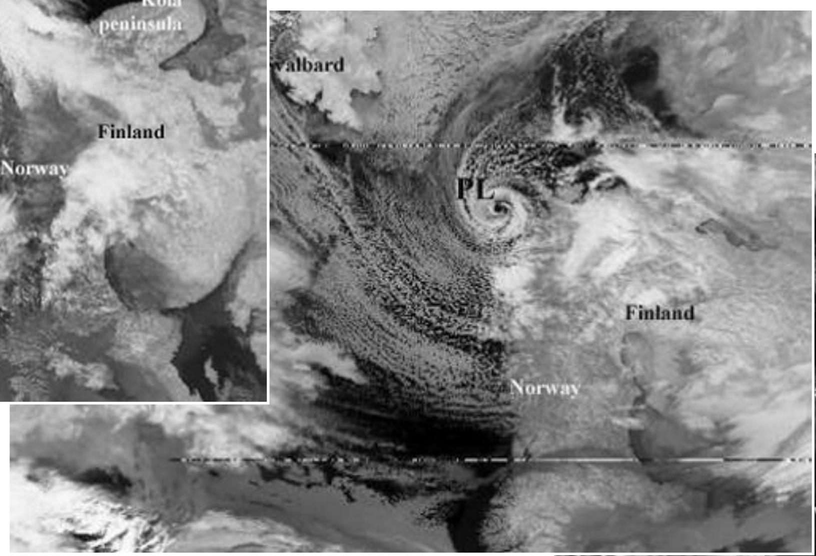

**Decaying phase, 27 February 1987
12:32 UTC**

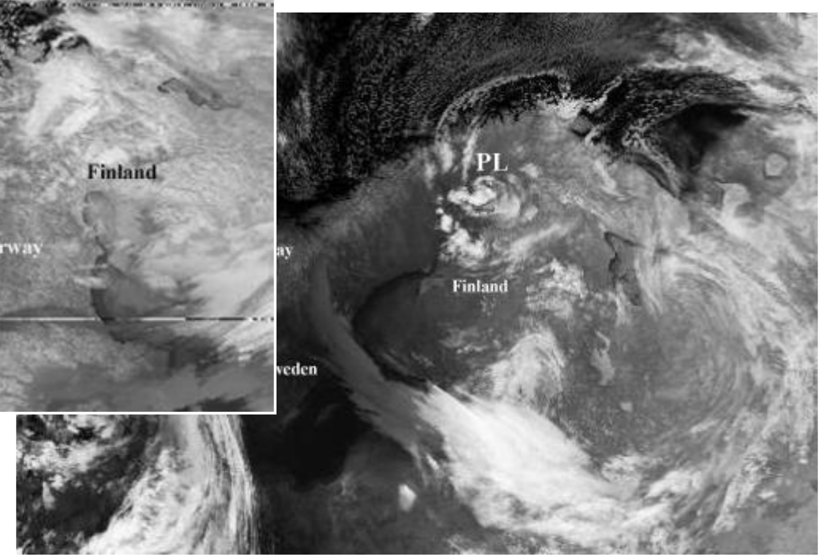

Satellite observations of polar lows with Synthetic Aperture Radar (SAR)

Satellite SAR advantages:

- Independence on day time
- Ability to see through clouds
- High spatial resolution
- High-resolution near-surface wind field retrieval
- Accurate location of atmospheric fronts and polar low centres at sea surface
- Indication of presence of small-scale organized variations of surface wind with various scales

Thus, SAR is powerful instrument for polar low study…

…however, it can not be used for polar low tracking due to long repeat times and scarcity of images

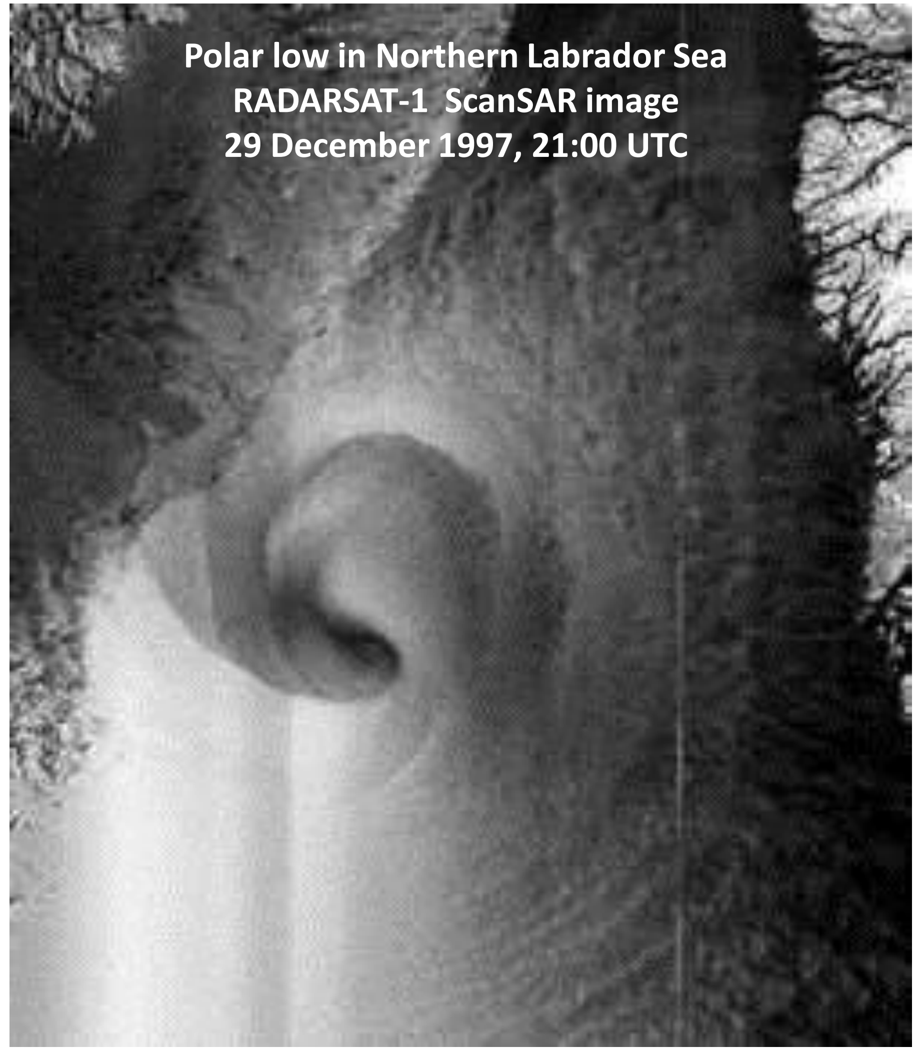

Satellite SAR – powerful instrument for polar low study

Wide swath SAR:
Envisat ASAR,
RADARSAT-1/2 SAR,
ALOS-1/1 PALSAR,
RISAT SAR,
Sentinel
can contribute
to polar low studies

Envisat ASAR images

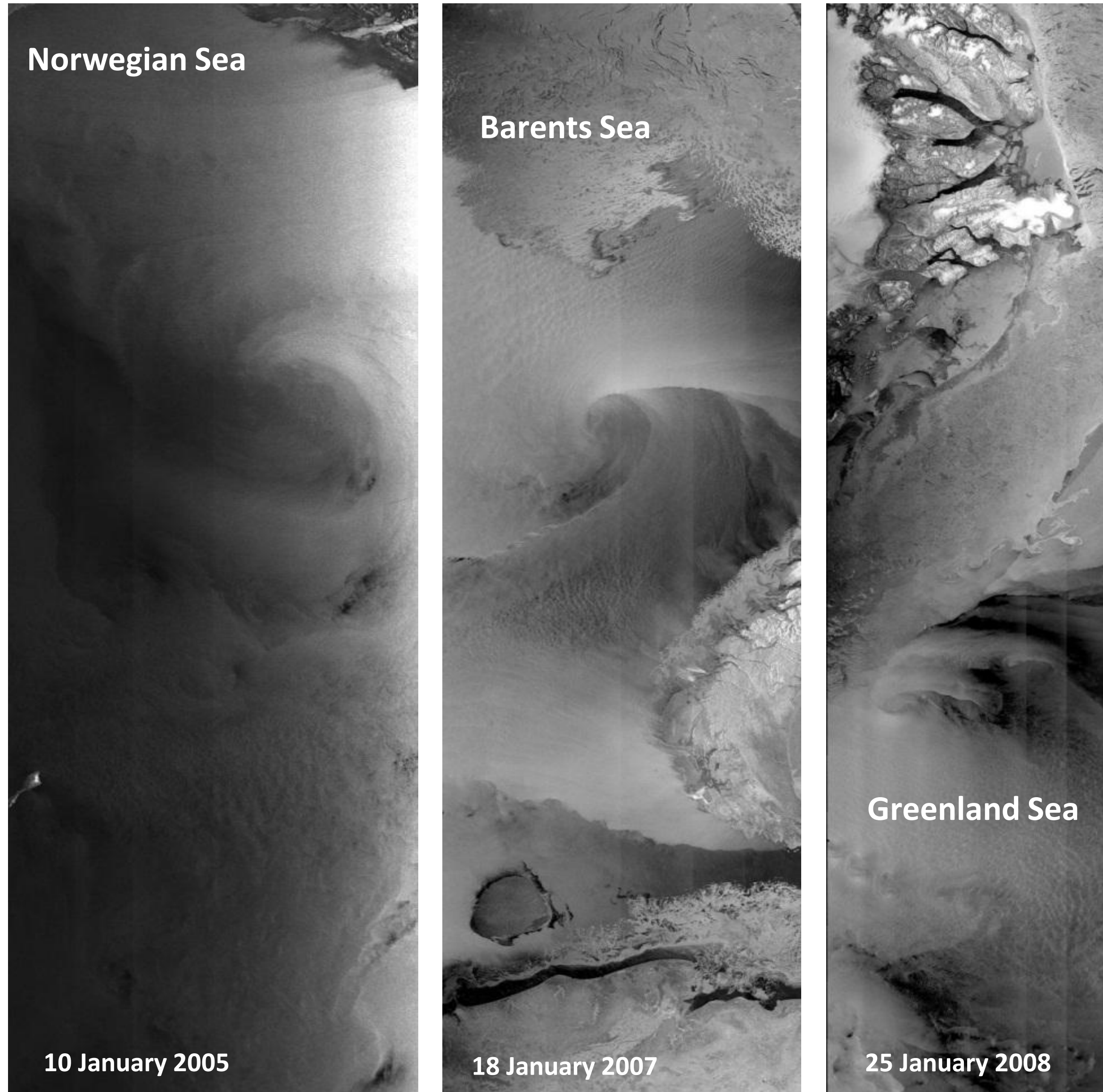

Satellite observations of polar lows with passive microwave radiometers

Advantages:

- independent on day time
- independent on clouds
- regularity and high temporal resolution in polar region

Retrieved parameters:

- sea surface wind speed
- atmospheric columnar water vapor
- total cloud liquid water content
- sea surface temperature (AMSR-E)

Satellite	Radiometer	Period of data availability
Nimbus-7 - US	Scanning Multichannel Microwave Radiometer (SMMR)	1978-1987
Defense Meteorological Satellite Programme (DMSP) - US	Special Sensor Microwave Imager (SSM/I)	1987-2009
Aqua - US	Advanced Microwave Scanning Radiometer - Earth Observing System (AMSR-E)	2002 - 4 October 2011 (failed)
DMSP - US	3 radiometers: Special Sensor Microwave Imager / Sounder (SSMIS)	2005-now
Global Change Observation Mission – Water (GCOM-W1) – Shizuku - Japan	Advanced Microwave Scanning Radiometer AMSR2	Launched on 18 May 2012

31 January 2008 11:14 UTC

23.8 GHz, V

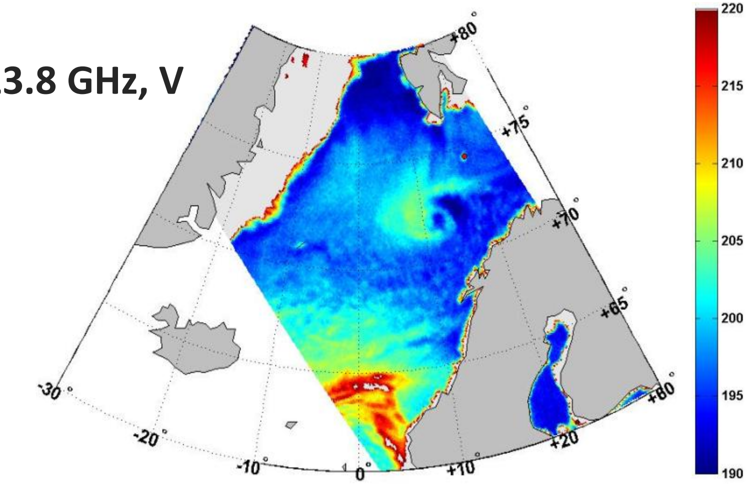

36.5 GHz, H

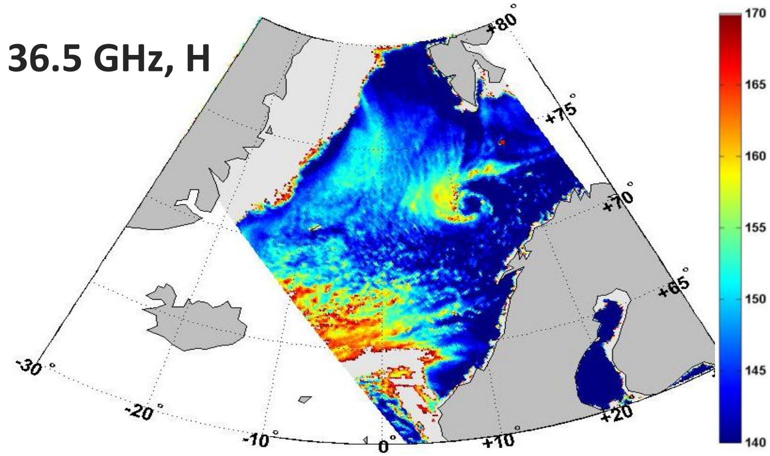

Fields of brightness temperatures measured by AMSR-E

General approach for polar low detection and tracking using satellite passive microwave data

- Retrieval of atmospheric columnar water vapor fields from satellite passive microwave data (e.g., SSM/I and AMSR-E)
- Detection of vortex structures in these fields
- Polar low parameter (life time, size, location, moving speed) estimation and trajectory tracking

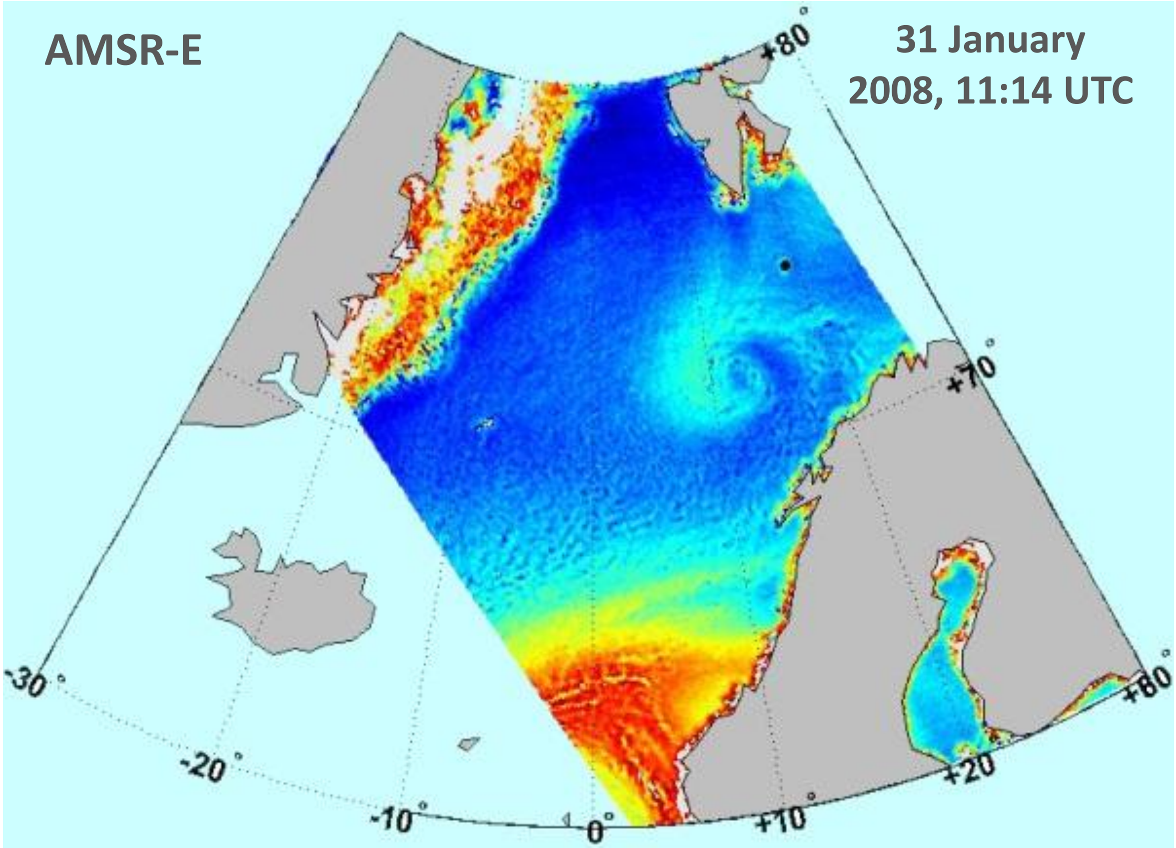

Bobylev et al., IEEE TGRS, 2010 **– NN-algorithm for columnar water vapor retrieval**
Bobylev et al., IEEE TGRS, 2011 **– polar low detection and tracking approach**

Nansen International Environmental and Remote Sensing Centre
NIERSC

Case study 1: Polar low tracking over the Norwegian Sea from SSM/I and AMSR-E 30-31 January 2008

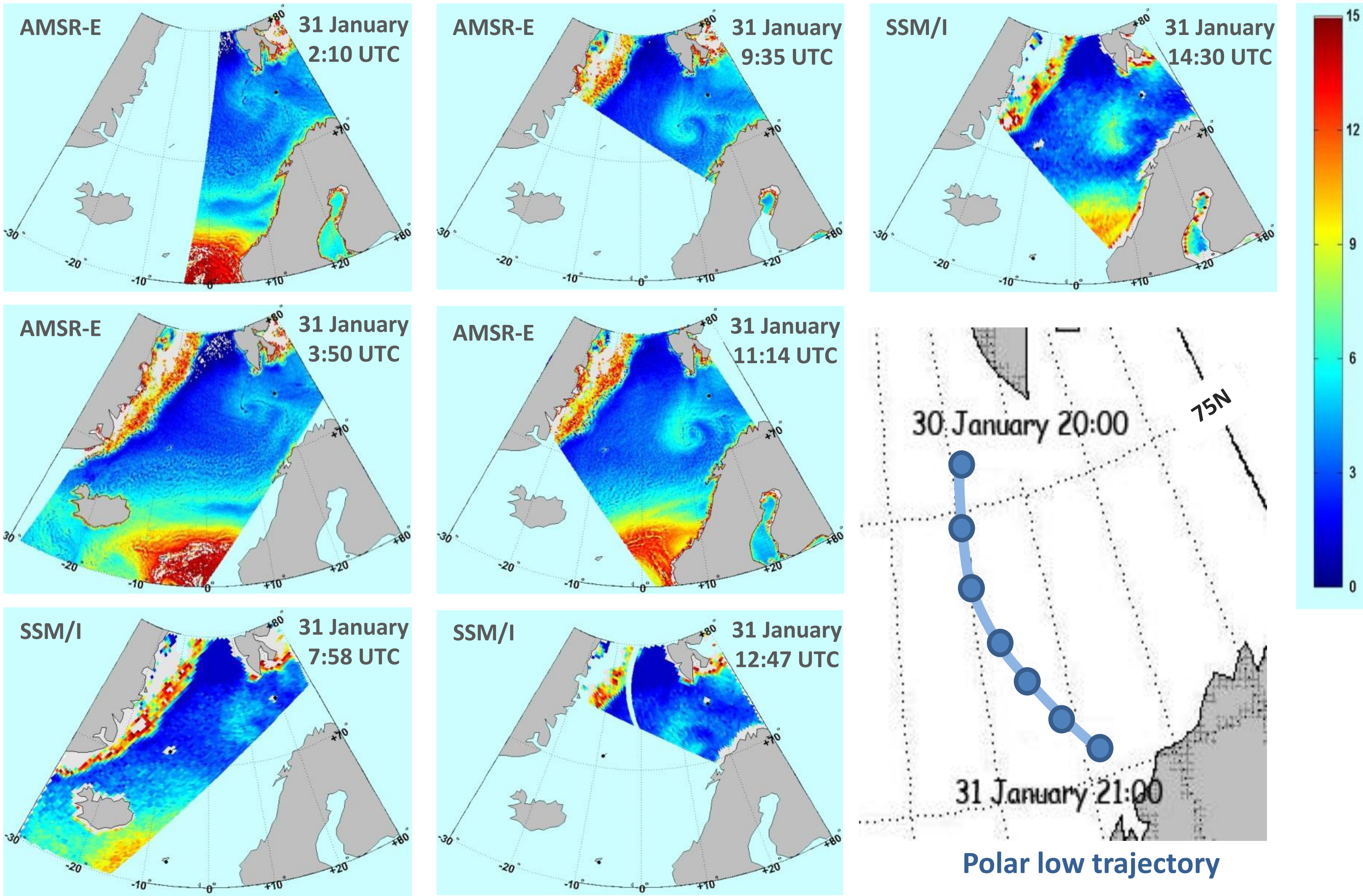

Polar low trajectory

Case study 1: Polar low over the Norwegian Sea 30-31 January 2008 (continuation)

Comparison of AMSR-E detected polar low with IR image

AMSR-E
31 January
9:35 UTC

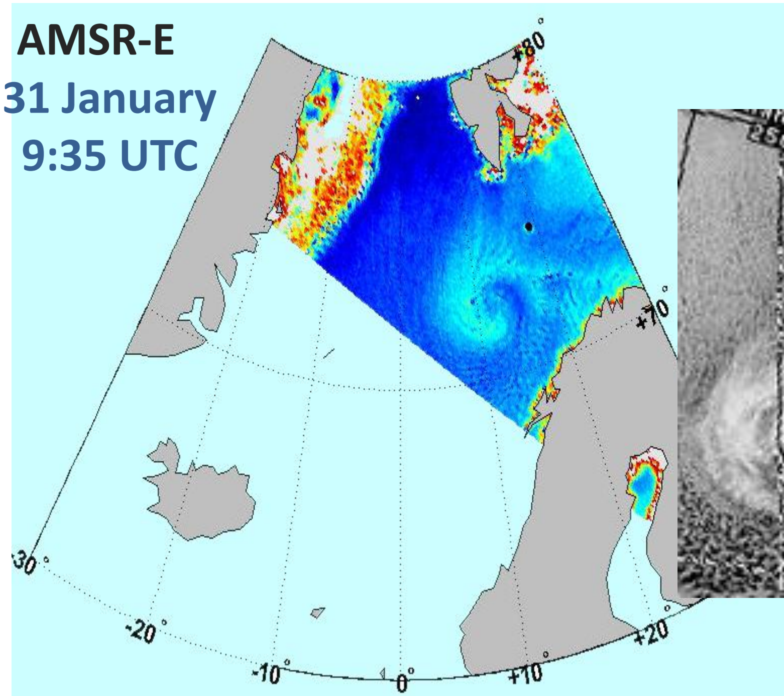

AVHRR NOAA image (10.3-11.3 µm, 4 ch)
31 January 10:11 UTC

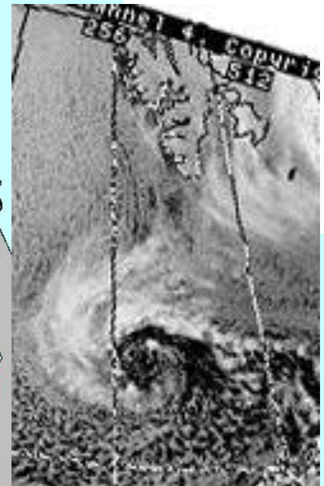

AMSR-E
31 January
11:14 UTC

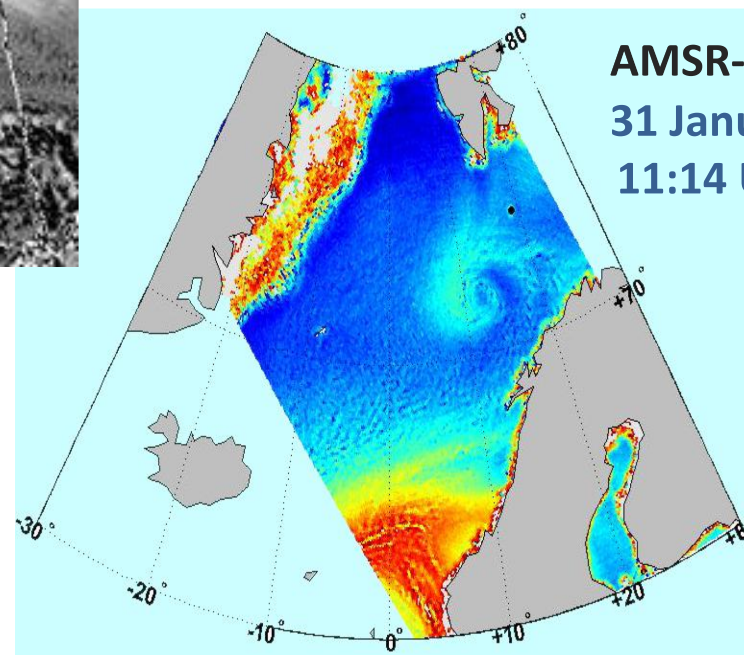

Case study 1: Polar low in the Norwegian Sea 30-31 January 2008 (continuation)

Comparison of AMSR-E detected polar low with surface wind field from scatterometer data

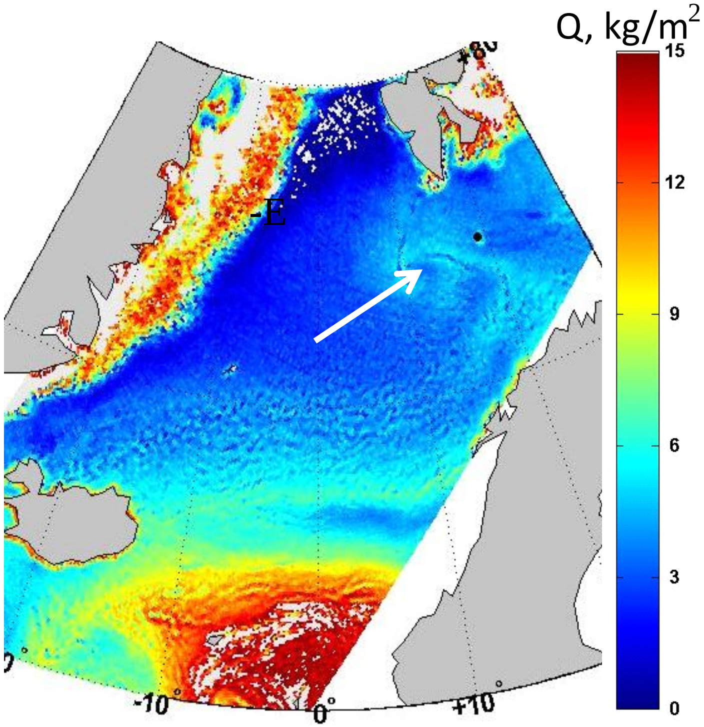

AMSR-E retrieved columnar water vapor (Q) field (31 January, 03:50 UTC)

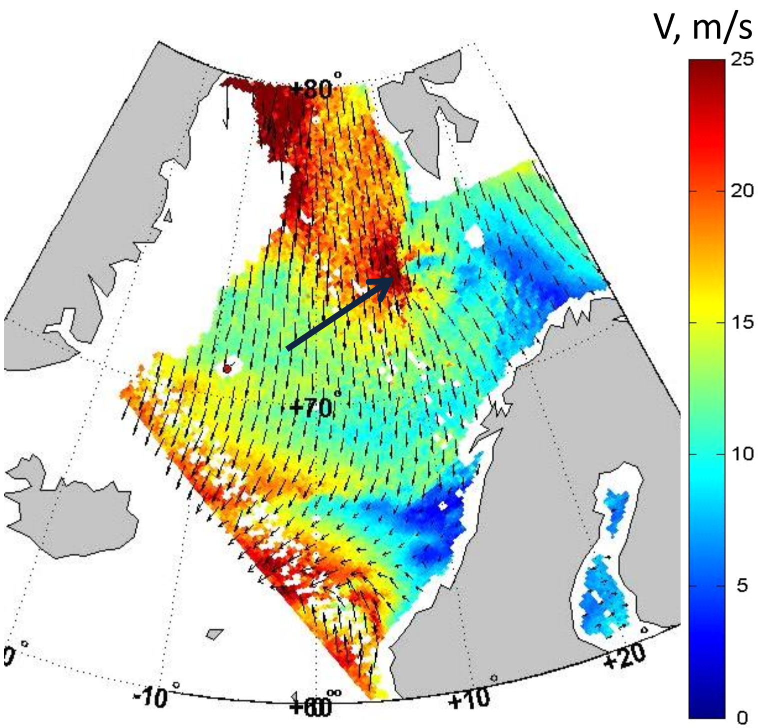

QuikSCAT sea surface wind speed (V) field (31 January, 03:40 UTC)

Case study 2: Polar low tracking over the Barents Sea from SSM/I and AMSR-E 7-8 January 2009

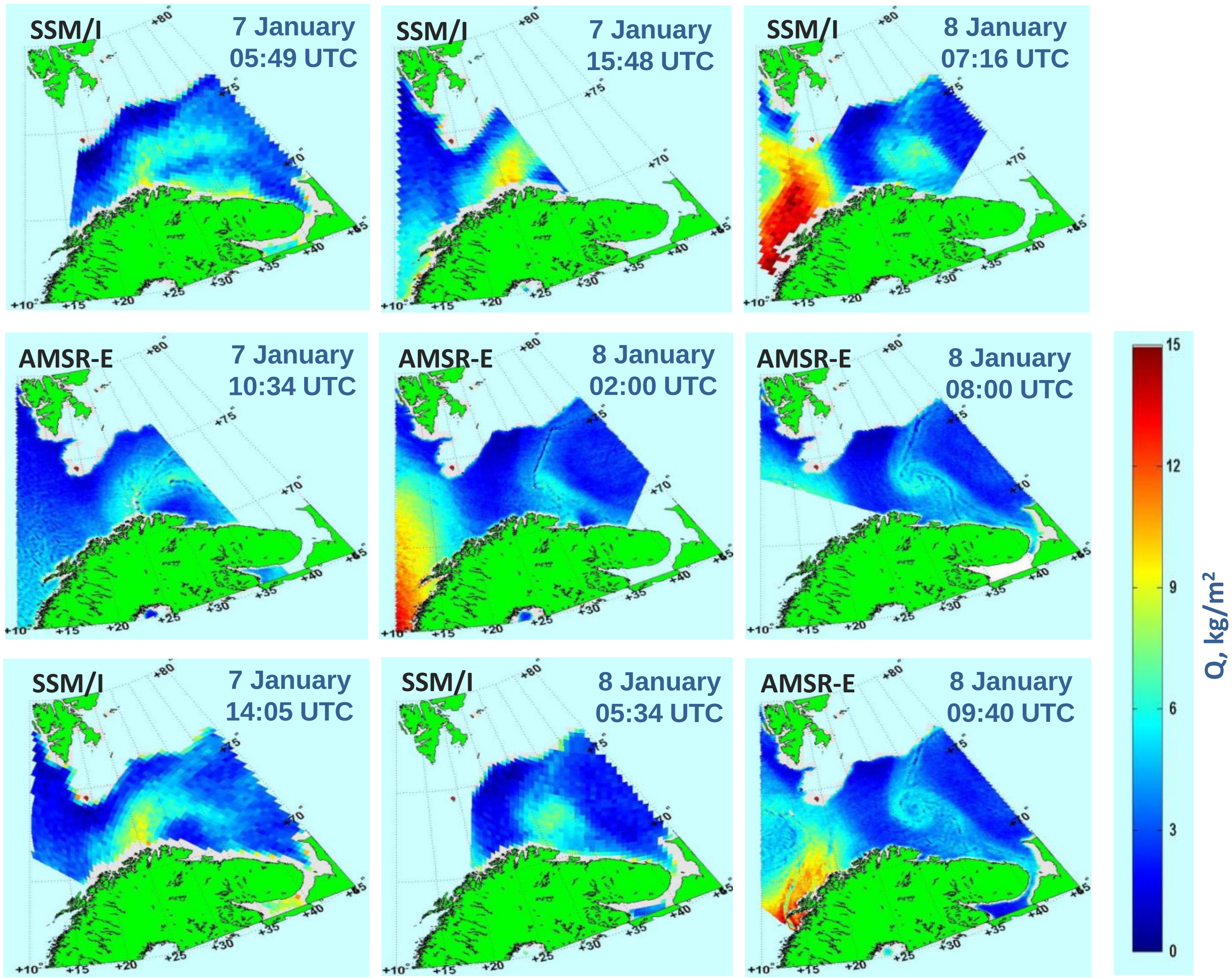

Case study 2: Polar low in the Barents Sea 7-8 January 2009 (continuation)

Comparison of AMSR-E detected polar low with MODIS image and high-resolution surface wind field from ENVISAT ASAR

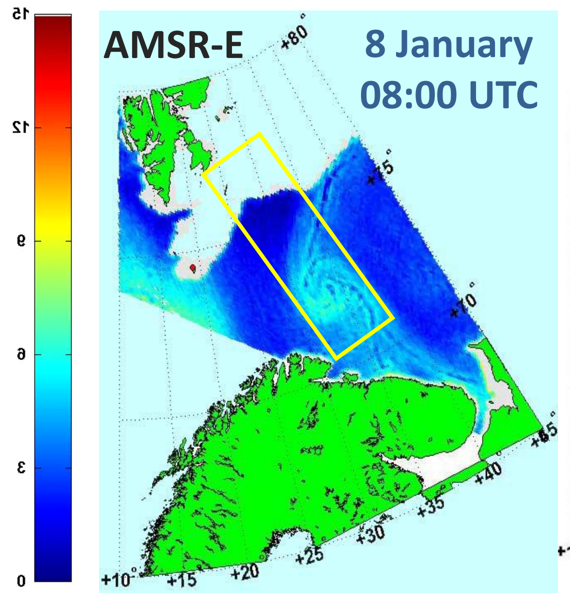

AMSR-E retrieved columnar water vapor (Q) field

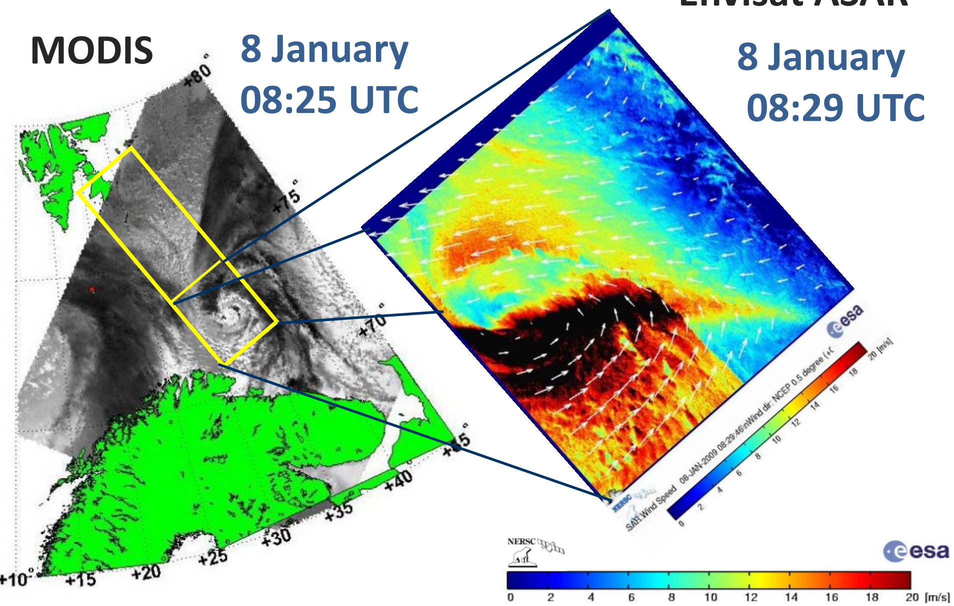

ENVISAT ASAR wind retrieved with CMOD4

Existing polar low climatologies

Year	Paper	Period	Type of data	Area	Method
2011	G. Noer, Ø. Saetra, T. Lien, Y. Gusdal (2011). A climatological study of polar lows in the Nordic Seas. *Quarterly Journal of the Royal Meteorological Society*, **137**(660), 1762–1772	2000-2009	Visible imagery	Nordic Seas	Subjective analysis
2008	Zahn, M., and H. von Storch (2008). A longterm climatology of North Atlantic polar lows. *Geophys. Res. Lett.*, **35**, L22702, doi:10.1029/2008GL035769	1948 - 2006	Model: NCEP/NCAR re-analyses data and CLM data	Sub-Arctic region of the North Atlantic	Objective analysis of pressure fields using digital filter
2008	Blechschmidt, A.-M. (2008). A 2-year climatology of polar low events over the Nordic Seas from satellite remote sensing. *Geophys. Res. Lett.*, **35**, L09815, doi:10.1029/2008GL033706	2004 - 2005	Combined use of thermal infrared AVHRR imagery and SSM/I derived wind speeds from HOAPS	Nordic Seas	Subjective analysis
2008	Thomas J. Bracegirdle*, Suzanne L. Gray. (2008). An objective climatology of the dynamical forcing of polar lows in the Nordic seas. *Int. J. of Climatol.*, **14**(28), 1903-1919	January 2000 to April 2004	Cyclone Database developed by Hewson objectively identified from the UK Met Office global operational model	Norwegian and Barents seas	Objective analysis
2006	Kolstad, E.W. (2006). A new climatology of favorable conditions for reverse-shear polar lows. *Tellus*, **58A**, 344–354	1948 - 2005	Model: ERA-40 reanalysis data	Latitudes over 60°N	Objective analysis
1999	Harold, J.M., Bigg, G.R. and Turner, J. (1999). Mesocyclone activities over the north-east Atlantic. Part 1: vortex distribution and variability. *Int. J. Climatol.* ,**19,** 1187–1204	October 1993- Sept 1995	Infrared AVHRR	North-East Atlantic and Nordic Seas	Subjective analysis -eye inspection
1985	Wilhelmsen, K. 1985. Climatological study of gale-producing polar lows near Norway. *Tellus*, **37A**, 451–459	1972-1977	Weather maps	Norwegian and Barents seas	Subjective analysis

A long-term climatology (1948-2006) of North Atlantic polar lows
(Matthias Zahn and Hans von Storch, GRL, 2008)

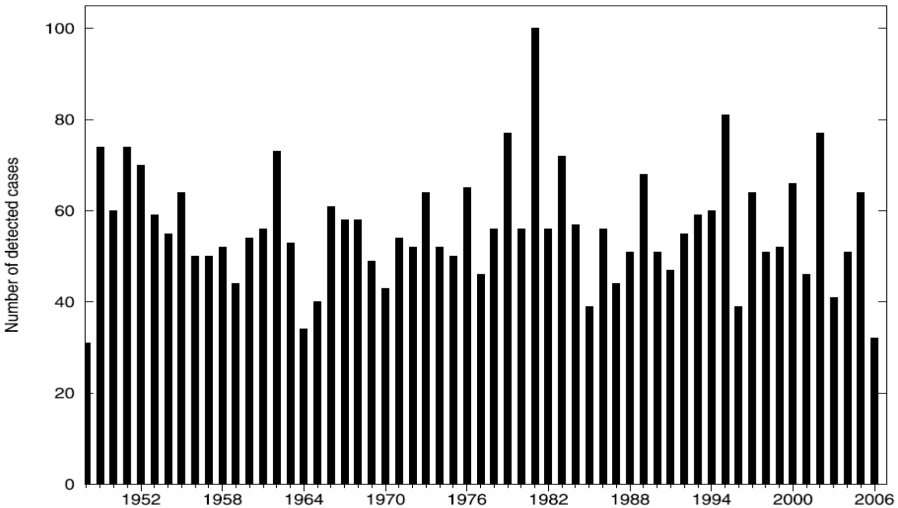

Number of detected polar lows per polar low season

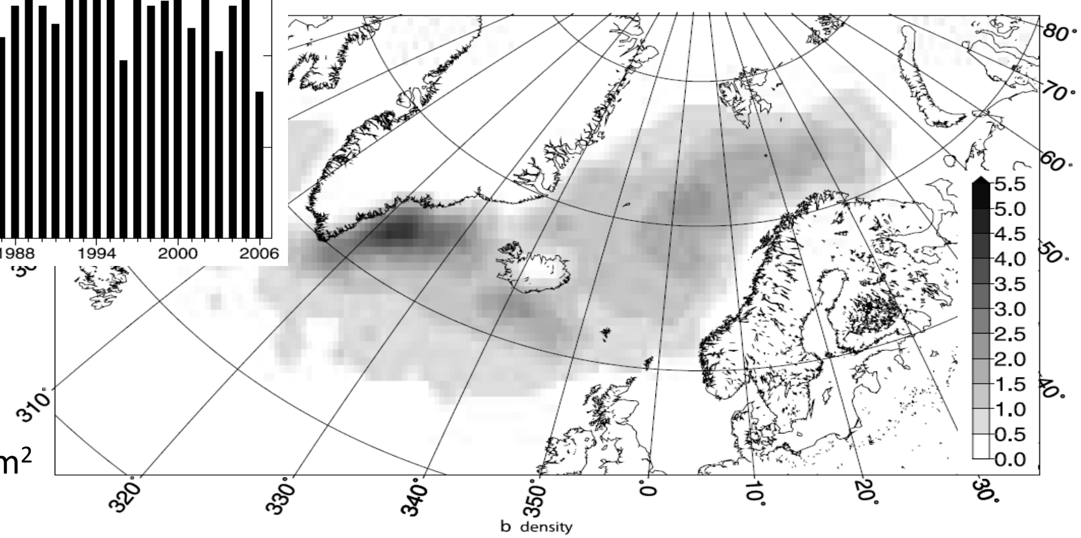

Polar low density distribution.
Unit: detected polar lows per 250 km^2

- Large interannual but little decadal variability of polar low occurrence
- No significant long-term trends in overall or regional polar low activity

Comments to Zahn-von Storch climatology

- Mesoscale cyclones/polar lows are under-represented in current reanalysis datasets *(Condron et al., 2006)*:
  - up to 80 % of cyclones larger than 500 km can be detected in mean sea level (MSL) pressure
  - up to 40 % - for 250-km-scale cyclones, and
  - only 20 % - for 100-km-scale cyclones
- Modal size of AVHRR-derived mesoscale cyclones/polar lows is 100-150 km *(Harold et al., 1999)*

Creating polar low climatology for the Nordic Seas over 1995-2011 based on atmospheric water vapor field analysis

Data	Period	Purpose	Comments
Satellite passive microwave: DMSP SSM/I, SSMIS	1995-2011	Atmospheric columnar water vapor field retrieval and vortex structure identification, polar low parameter estimation, trajectory tracking	Well calibrated data are unavailable before 1995
Satellite scatterometer: QuikSCAT SeaWinds Metop ASCAT	2002-2009 (SeaWinds) 2009-2011 (ASCAT)	Polar low detection confirmation by means of surface wind speed field analysis (presence of high wind speeds)	Few scarce data from ERS-1/2 and NSCAT before 1995
Envisat ASAR	2005-2011	Study of polar low manifestation in the sea surface wind field vortex structure, PL case studies	The highest resolution. Scarce and rare data
Aqua and Terra MODIS NOAA AVHRR IR and visible images	2002-2011 (MODIS) 1995-2011 (AVHRR)	Cloud structure analysis, PL case studies	
NCEP/NCAR re-analysis	1995-2011	Geopotential filed analysis, comparison with results obtained from water vapor field study	

Polar low over the Barents Sea on 27 January 2010

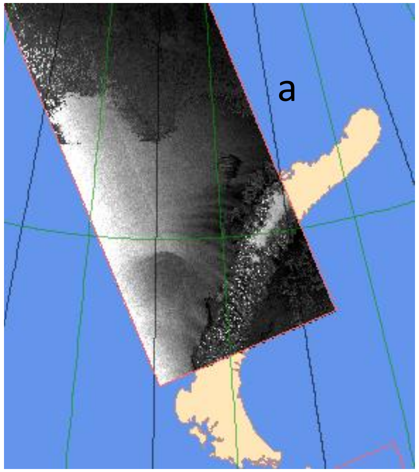

Envisat ASAR image
27 January 2010, 17:15 UTC

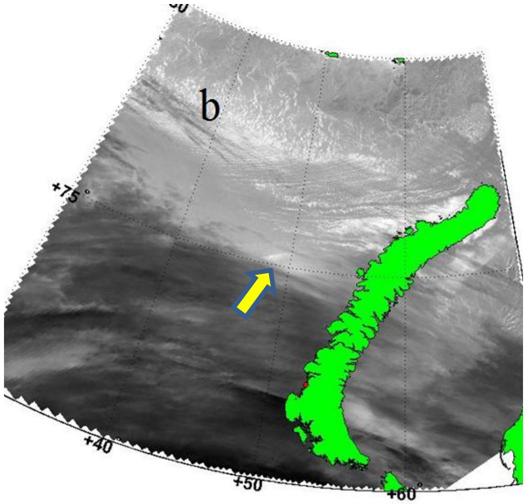

Terra MODIS infrared (10.78-11.28 μm) image 27 January 2010, 16:10 UTC

Malye Karmakuly station

10.7 kg/m^2 at 00 UTC

12.7 kg/m^2 at 12 UTC

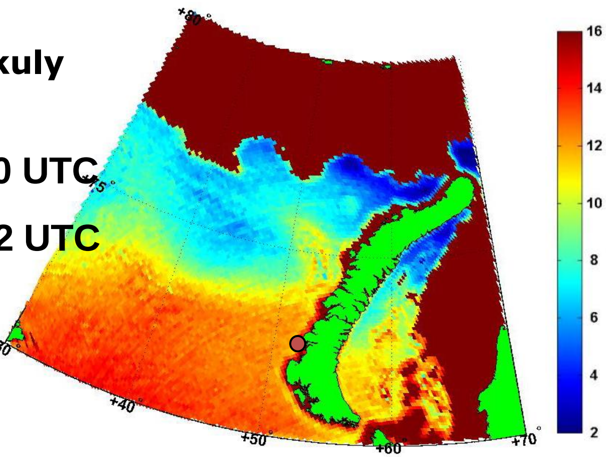

Total atmospheric water vapor content (Q) retrieved from Aqua AMSR-E 27 January 2010, 16:15 UTC

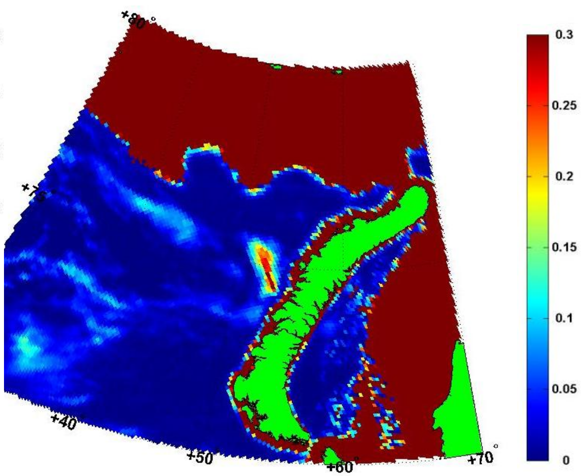

Total cloud liquid water content (W) retrieved from Aqua AMSR-E 27 January 2010, 16:15 UTC

Polar low over the Barents Sea on 5 March 2010

Aqua AMSR-E

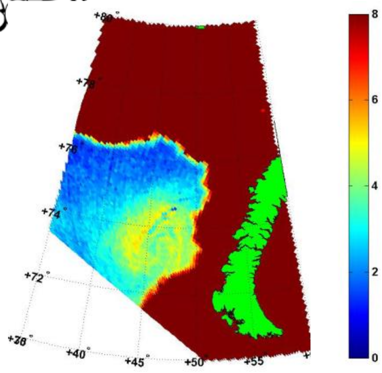

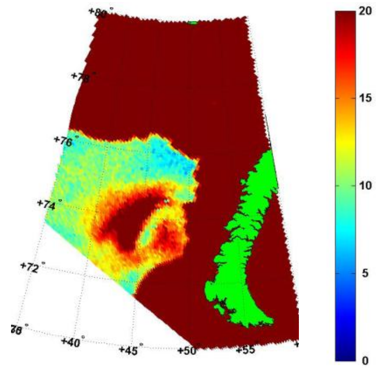

6:45 UTC Q, kg/m²

Total water vapor content

6:45 UTC V, m/s

Wind speed

Metop ASCAT

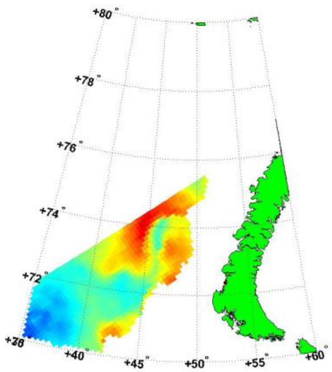

9:45 UTC

Wind speed

Terra MODIS

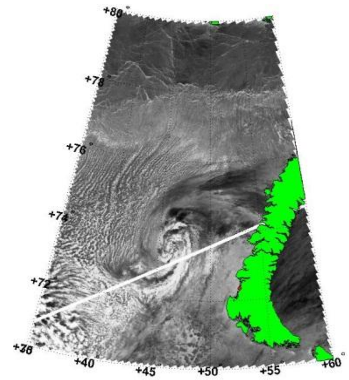

8:40 UTC

Cloud structure

NCEP/NCAR

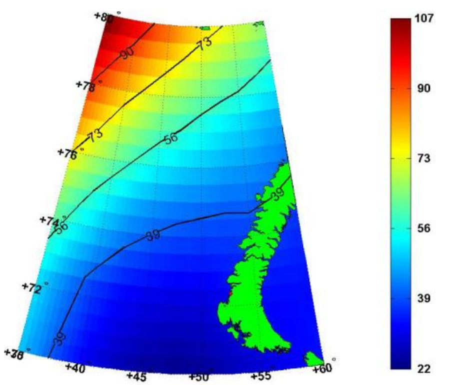

6:00 UTC

Geopotential, m2/s2

Geopotential

Envisat ASAR

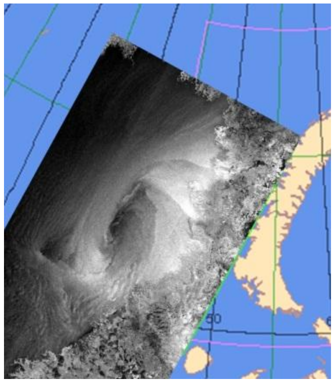

05:00 UTC

NOAA-16 AMSU-B

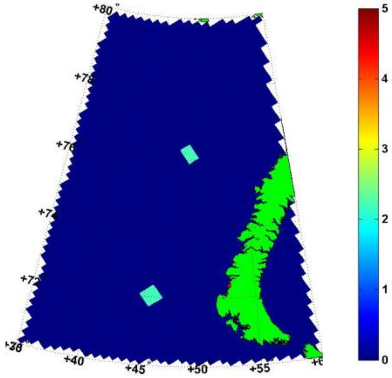

RR, mm/hr

13:00 UTC

Rain rate

Polar low over the Barents Sea
5 March 2010

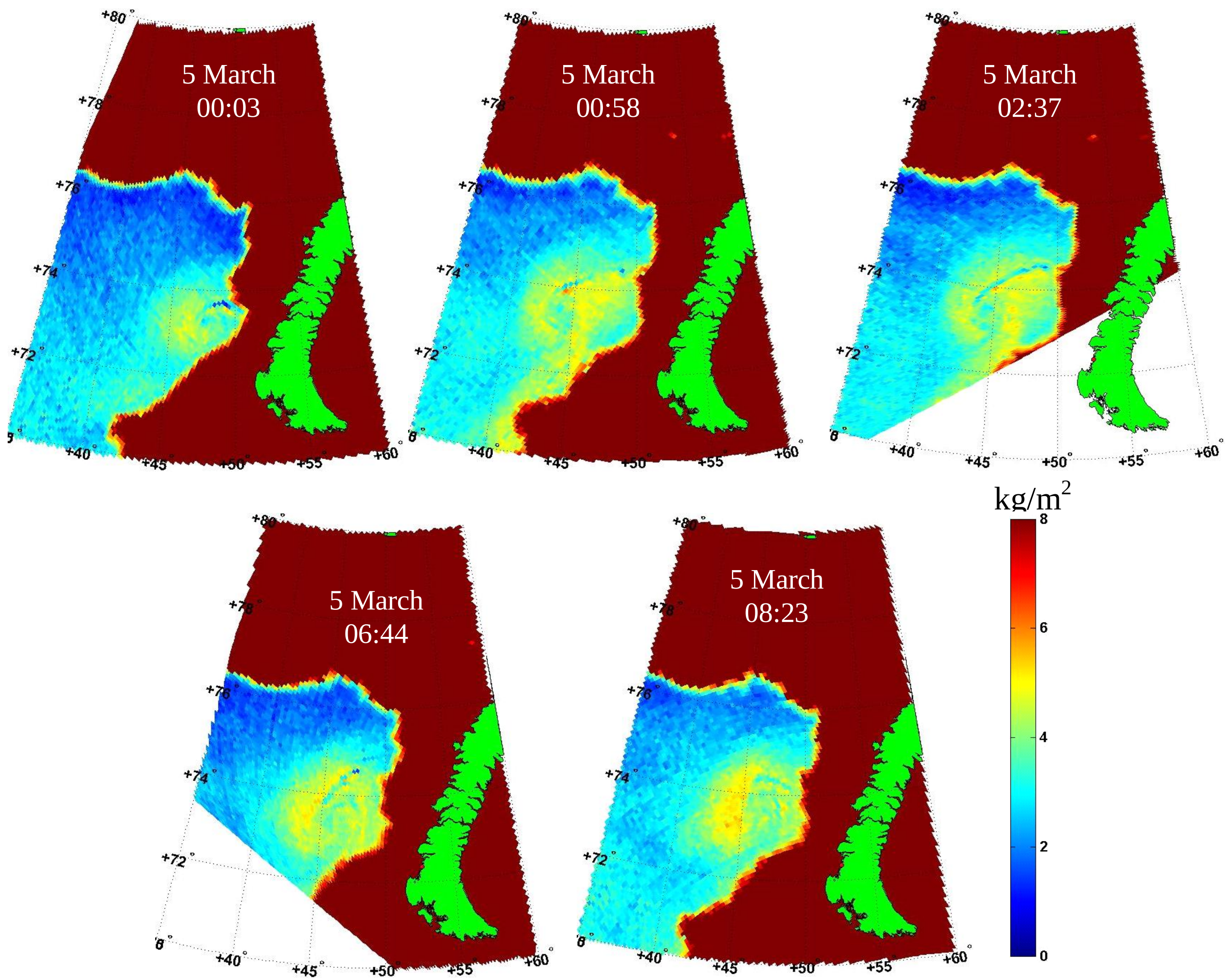

Total atmospheric water vapor content retrieved from Aqua AMSR-E

12 March 2011, two polar lows south to Spitsbergen

Terra and Aqua MODIS

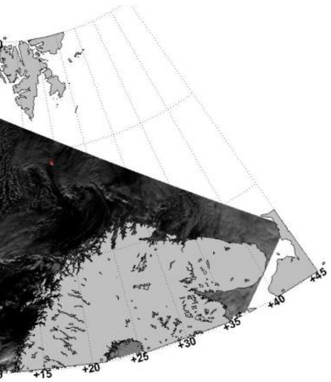

11:15 UTC

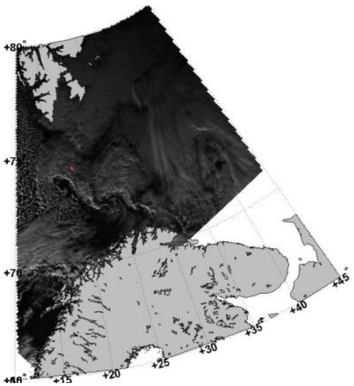

12:50 UTC

NCEP/NCAR

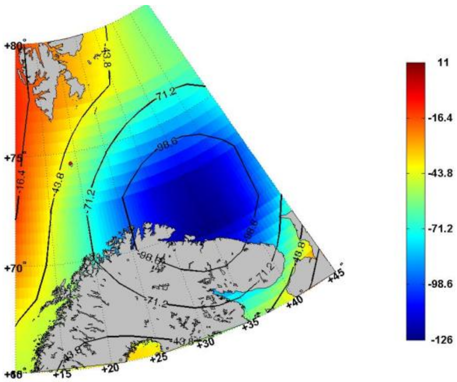

12:00 UTC Geopotential, m^2/s^2

Metop ASCAT

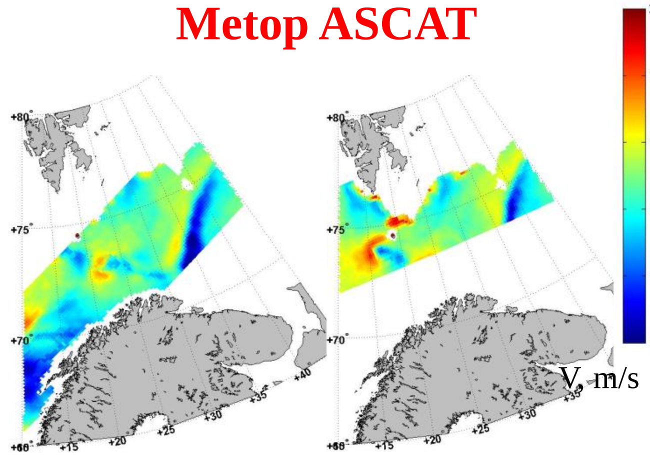

11:32 UTC 13:09 UTC

V, m/s

Envisat ASAR

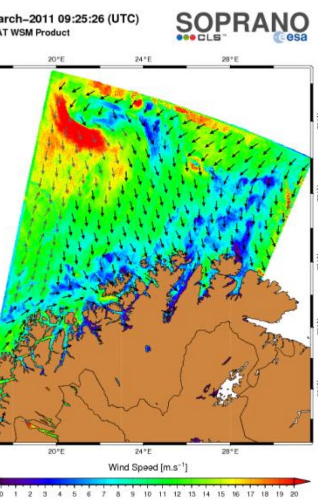

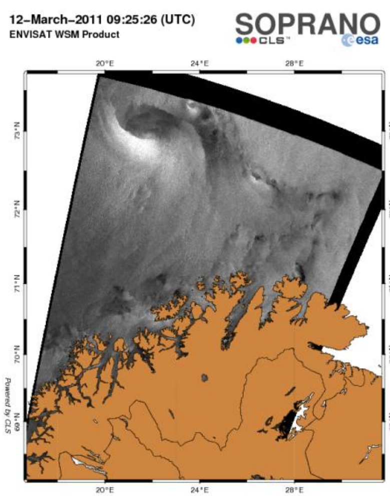

Aqua AMSR-E

11:35 UTC

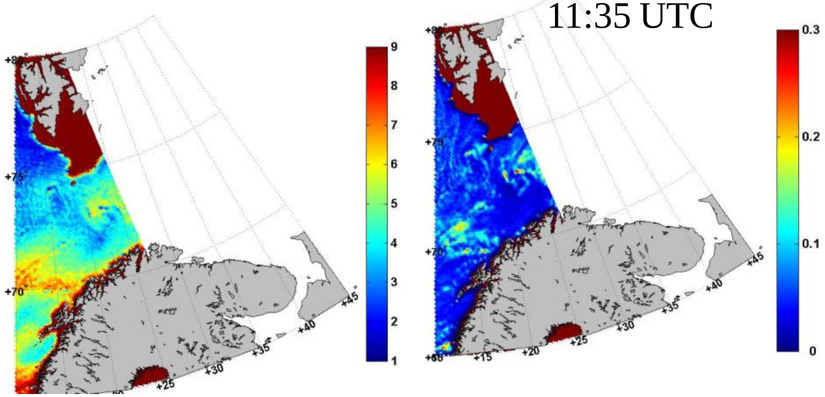

Water vapor content Q, kg/m^2 Cloud liquid water W, kg/m^2

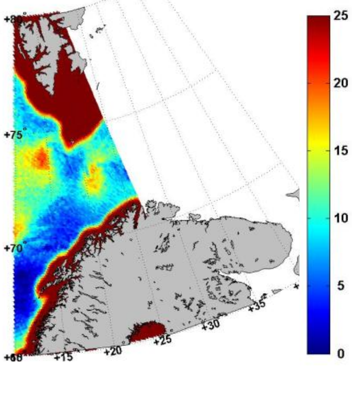

Surface wind speed

Aqua AMSR-E 8:17 UTC

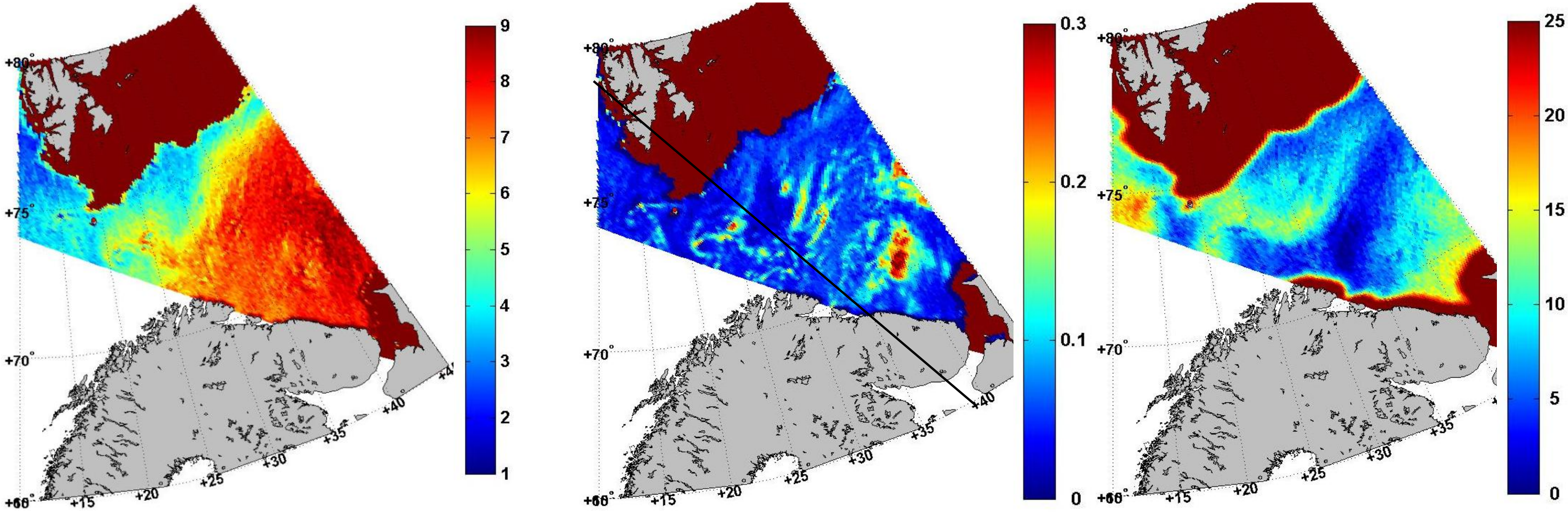

Water vapor content kg/m²

Cloud liquid water kg/m²

Surface wind speed m/s

12 March 2011: water vapor content over Bjornoya island:

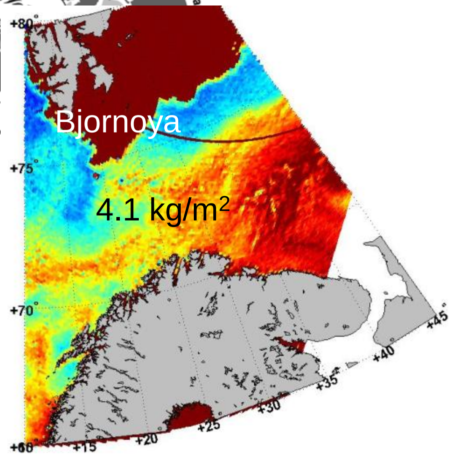

01:35 UTC

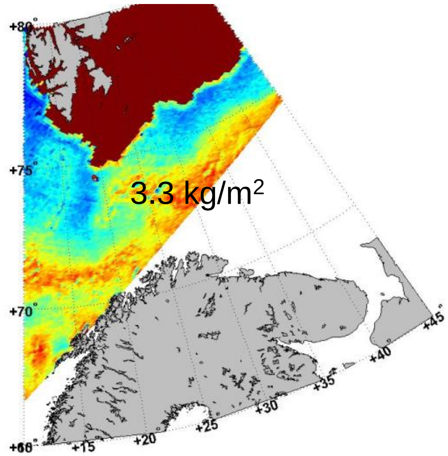

03:29 UTC

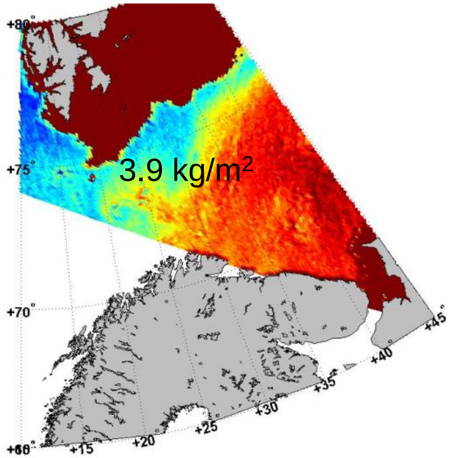

08:17 UTC

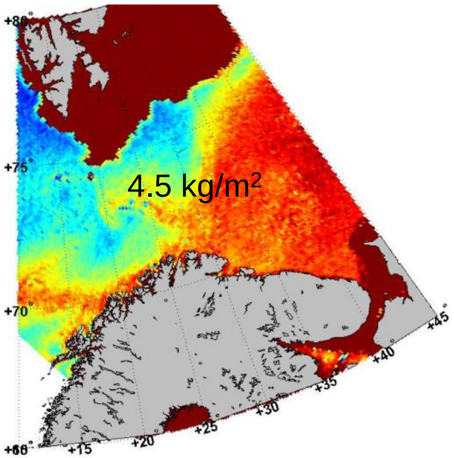

09:56 UTC

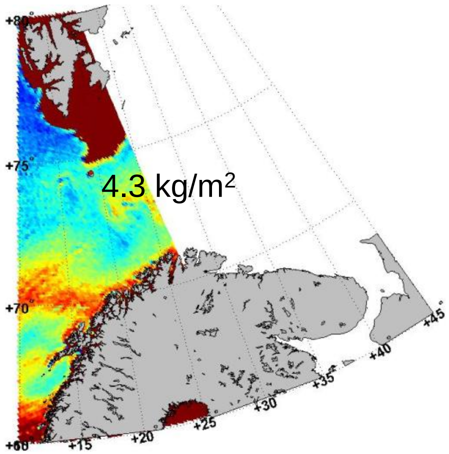

11:35 UTC

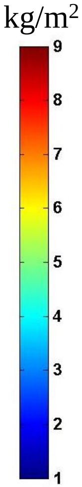

Bjornoya station radiosounding observation data:

00:00	4.35 kg/m^2
06:00	3.53 kg/m^2
12:00	4.01 kg/m^2
18:00	3.59 kg/m^2

Starting from 1 January 2010
4 radiosoundings per day

Surface Analysis Maps from German National Meteorological Service

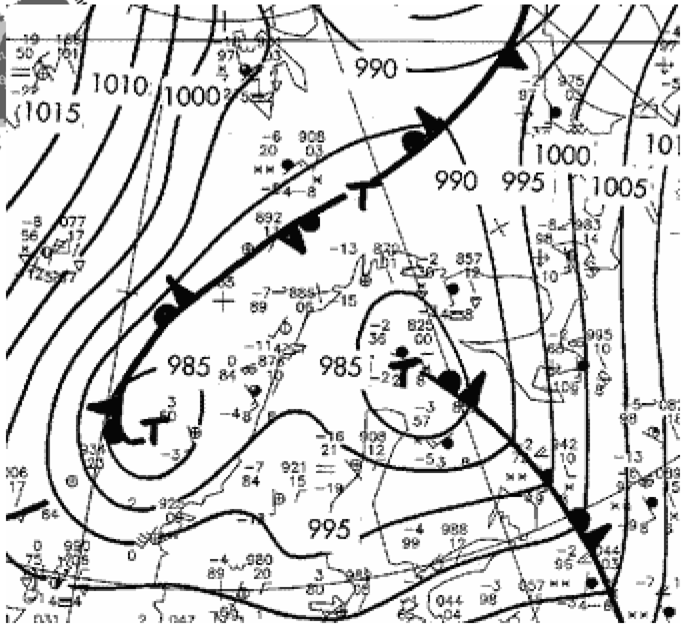

00:00 UTC

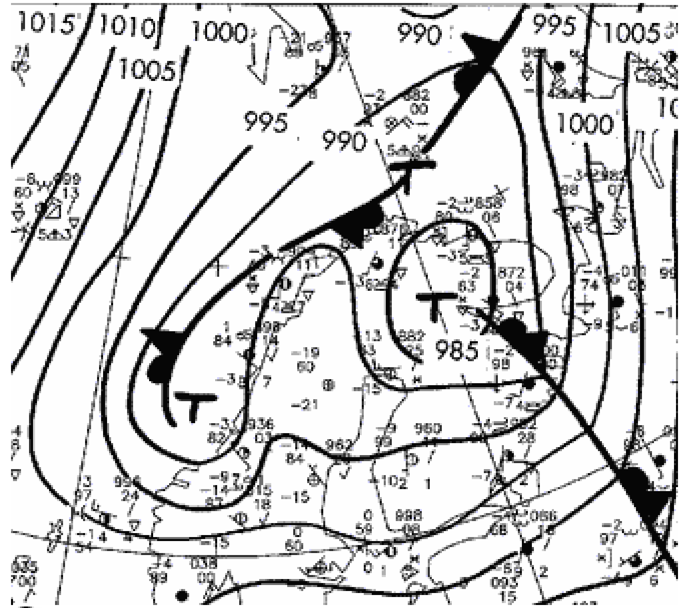

06:00 UTC

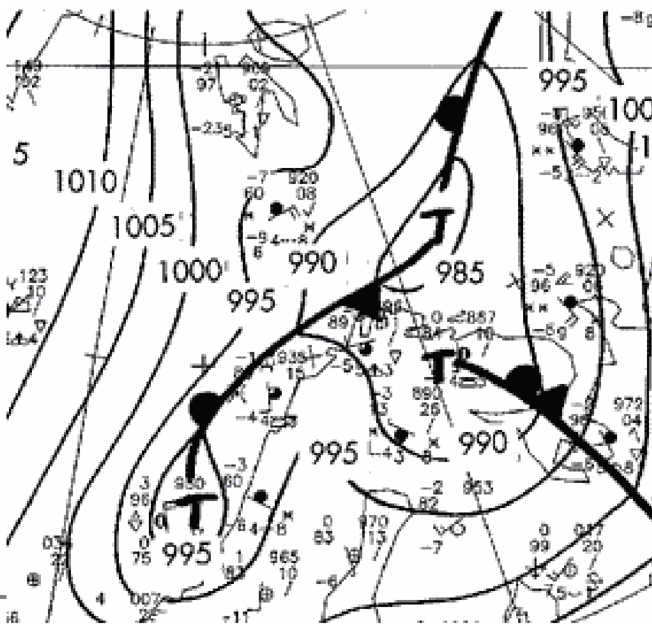

12:00 UTC

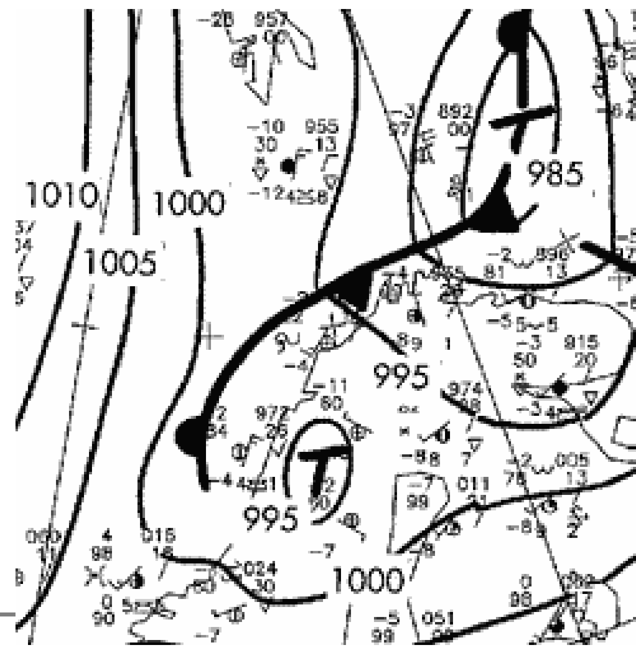

18:00 UTC

WRF - The Weather Research and Forecasting hydrodynamic mesoscale model. It was created through a partnership that includes the NOAA, NCAR and more than 150 other organizations and Universities in the United States and abroad.

Barents Sea

Three levels of nests,
with nest d01 acting as the parent for nest d02
and nest d02 acting as the parent for nest d03

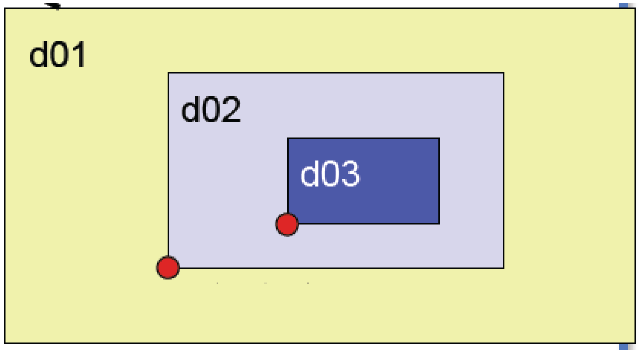

d01 grid - 100 x 100 points, space step 10 km, time step 60 s
d02 grid - 100 x 100 points, space step 3 km, time step 20 s
d03 grid - 100 x 100 points, space step 1 km, time step 6 s

Forecast fields – see level pressure and water vapor 9.01.2009